Layer-by-Layer-Coated Gelatin Nanoparticles as a Vehicle for Delivery of Natural Polyphenols

Tatsiana G. Shutava,[†,§] Shantanu S. Balkundi,[†] Pranitha Vangala,[†] Joshua J. Steffan,[‡] Rebecca L. Bigelow,[‡] James A. Cardelli,[‡] D. Patrick O'Neal,[†] and Yuri M. Lvov[†,*]

[†]Institute for Micromanufacturing and Biomedical Engineering Program, Louisiana Tech University, Ruston, Louisiana 71272, and [‡]Department of Microbiology and Immunology and the Feist-Weiller Cancer Center, Louisiana State University Health Sciences Center, Shreveport, Louisiana 71130. [§]Current address: Institute of Chemistry of New Materials, NASB, Minsk, Belarus.

ABSTRACT Natural polyphenols with previously demonstrated anticancer potential, epigallocatechin gallate (EGCG), tannic acid, curcumin, and theaflavin, were encased into gelatin-based 200 nm nanoparticles consisting of a soft gel-like interior with or without a surrounding LbL shell of polyelectrolytes (polystyrene sulfonate/polyallylamine hydrochloride, polyglutamic acid/poly-L-lysine, dextran sulfate/protamine sulfate, carboxymethyl cellulose/gelatin, type A) assembled using the layer-by-layer technique. The characteristics of polyphenol loading and factors affecting their release from the nanocapsules were investigated. Nanoparticle-encapsulated EGCG retained its biological activity and blocked hepatocyte growth factor (HGF)-induced intracellular signaling in the breast cancer cell line MBA-MD-231 as potently as free EGCG.

KEYWORDS: (−)-epigallocathechin gallate · EGCG · tannic acid · theaflavin · gelatin nanoparticles · layer-by-layer assembly · polyelectrolytes · encapsulation and release · HGF · intracellular signaling · tumor cells

Complex natural polyphenolic compounds are of great interest as substances possessing a high spectrum of biological activity. High antioxidant, antibacterial, antiviral, and other activities have been proven for a wide range of plant extracts and polymeric tannins including their isolated individual compounds (procyanidin B, tannic acid (TA), theaflavin (TF), thearubigins, *etc.*).[1−3]

Green tea polyphenols, such as epigallocatechin gallate (EGCG) and epicatechin gallate, have recently been demonstrated to be effective cancer chemopreventive agents in animal studies, and recent data from human clinical trials suggest tea polyphenols can slow the progression of prostate cancer or lower biological activities of proteins promoting cancer progression.[4−6] Other polyphenols such as curcumin,[4] luteolin,[5] resveratrol, and several others are under intensive investigation as possible anticancer agents.[6] Therefore, a large body of preclinical research and epidemiological data support the hypothesis that plant phytochemicals can act as chemopreventive and anticancer agents in humans. Unfortunately, concentrations that appear effective in blocking tumor cell proliferation or inducing apoptosis *in vitro* are often an order of magnitude higher than levels measured *in vivo*.

Therefore, one of the problems of using polyphenols to treat cancer is their potentially low bioavailability and short half-life. One alternative to using free compounds is to use polyphenol-loaded nanoparticles.[7−9] However, widely varying structures of the compounds, their moderate solubility, and fast oxidation under basic conditions[1−3,10−14] create additional challenges for encapsulation. Formation of nanocomplexes *via* polyphenol/protein binding,[10−14] alternated layer-by-layer assembly of polyphenols as films on planar support, or shells on microcores[15,16] has been proposed to produce micro- and nanoparticles containing the target substances. However, in several cases, it is difficult to control size, colloidal stability, and solubility of the nanoparticles as well as to design nanoparticles with a high concentration of the target polyphenol followed by its release in a controlled manner.

The flavonoid, (−)-epigallocatechin gallate (EGCG), originating from the plant *Camelia sinensis* is the major component of green tea extract and is highly soluble in aqueous buffers and several organic solvents. These properties make several commonly used methods of encapsulation unfeasible. According to the authors' knowledge, attempts to encapsulate EGCG in nanoparticles are limited to a PGLA nanoparticulate formulation used for *in vivo* evaluation of antioxidant efficacy of EGCG in a rat model[17] and chitosan-

*Address correspondence to ylvov@coes.latech.edu.

Received for review February 18, 2009 and accepted June 06, 2009.

Published online June 17, 2009.
10.1021/nn900451a CCC: $40.75

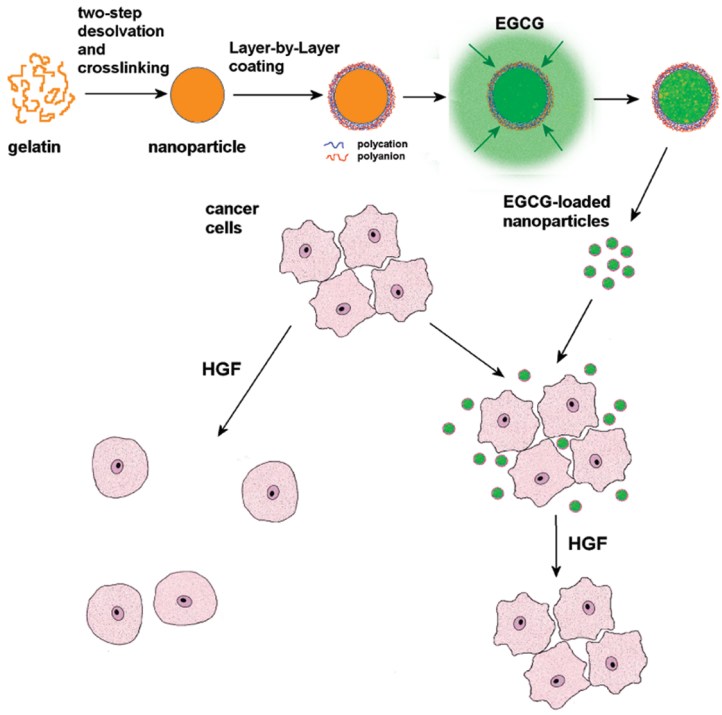

Figure 1. Schematic presentation of preparation of LbL-coated gelatin nanoparticles containing EGCG and their effect on cancer cells.

tripolyphosphate nanoparticles for encapsulation of green tea catechin extracts.[18]

Here we propose a first example of EGCG encasing into gelatin-based 200−300 nm nanoparticles consisting of a soft gel-like interior and a surrounding shell of polyelectrolytes (polystyrene sulfonate/polyallylamine hydrochloride (PSS/PAH), polyglutamic acid/poly-L-lysine (PGA/PLL), dextran sulfate/protamine sulfate (DexS/ProtS), carboxymethyl cellulose/gelatin, type A (CMC/GelA)) assembled using the layer-by-layer (LbL) technique[19−24] as shown in Figure 1. Gelatin-based nanoparticles have been proven to be relatively safe and effective nonviral gene delivery vehicles with a prolonged *in vivo* circulation time and high accumulation at the tumor side.[25−27] Modification of nanoparticle surfaces with polyelectrolyte LbL shells allows for modulating nanoparticle cell uptake rate and ratio, providing a template for their modification with tumor-targeting agents, increasing nanoparticle colloidal stability, and controlling loading/release characteristics.[20−24] EGCG is a well-known substance to reversibly react with hydrophobic moieties of proline-rich peptides, and this will provide loading/release characteristics in a pH-dependent manner.[28−32]

RESULTS AND DISCUSSION

Nanoparticle Preparation. To increase the strength of gel-like nanoparticles, gelatins with relatively higher Bloom numbers as compared with the original work of Coester,[33] 300 Bloom for gelatin A and 225 Bloom for gelatin B, were used in our study. In order to obtain a stable suspension of the nanoparticles with a minimal diameter, the procedure for gelatin nanoparticle preparation was slightly modified. Several essential parameters, such as temperature on the first and second desolvation stages, amounts of added reagents (acetone and gluteraldehyde), and the rates of their addition,[33] were set constant, while the pH value during the final stage of nanoparticle preparation varied in range from 1.5 to 5. At pH 4 and higher, the method produces unstable large nanoparticles of 700−750 nm diameters (Figure A, Supporting Information) which tend to precipitate very quickly. The suspensions of nanoparticles obtained at pH 3.0 are small and extremely stable. The diameter of the gelatin A nanoparticles is reproducibly around 200 nm. While the pH value decreases further, nanoparticle diameter increases to 300 nm and then to 400 nm. The nanoparticles prepared at these low pH values retain their stability at least for 4 weeks. The results are in good agreement with refs 33 and 34, where the pH range of 2.3−3.8 was recommended for the second desolvation stage. This coincides well with a sharp decrease in viscosity of gelatin aqueous solutions below pH 3 due to protonantion of aspartic and glutamic amino acid residues.[35] However, the observed minimum nanoparticle diameter was not previously reported and probably related to the higher Bloom numbers for the used gelatin. The hydrodynamic diameter of nanoparticles prepared from gelatin B at pH 3.0 is 127 nm. Nanoparticles of gelatin A prepared at pH 2.5−3.0 and gelatin B obtained at pH 3.0 were used for all further studies.

Characterization of Gelatin Nanoparticles. Both gelatin A and gelatin B nanoparticles have isoelectric points between pH 6 and 7 (Figure 2). The hydrodynamic diameter of the gelled nanoparticles slightly increases with increasing pH. The increase is 3.7 and 6.5 nm per one pH unit for gelatin A and gelatin B, respectively, and no large swelling or partial particle dissolution was observed even at pH 10. It points toward formation of relative inflexible cross-linked chain net in the nanoparticle interior.

According to AFM results, the effective diameter of dried gelatin B nanoparticles as prepared from 75% acetone is 120−150 nm (Figure 3a), values corresponding to the hydrodynamic diameter scattering of the nanoparticles (Figure A, Supporting Information). At the same time, while 300 nm gelatin A nanoparticles were deposited from an aqueous suspension and dried on a mica support, their average diameter appeared to be 367 ± 15 nm (Figure 3b,d) with the height of 58 ± 8 nm. The nanoparticles are collapsed and slightly deformed while dried. If we consider the shape of a dried nanoparticle as a cone and assume that density of the material is 1.1 g/cm^3,[24] the mass of one gelatin A nanoparticle is 2.3×10^{-15} g. If the nanoparticle's actual size is assumed to be equal to its hydrodynamic diameter, the gelatin nanoparticles consist of 15% solid gela-

tin while the remaining 85% is water. From here on, the dry gelatin material is referred to as solid material of a suspension, always being kept in mind that the nanoparticle's actual volume is about 5.7 times higher.

Layer-by-Layer Assembly of Polyelectrolytes on Gelatin Nanoparticles. Two combinations of polyanion/polycation pairs were used to form an LbL coating around 300 nm gelatin nanoparticles, PSS/PAH (strong polyanion/weak polycation) and PGA/PLL (weak polyanion/strong polycation) as well as two combinations of polyanion/protein, DexS/ProtS (strong polyanion/strongly positively charged polypeptide) and CMC/GelA (weak polyanion/weak positively charged protein).[19,20] At pH 6.0, the surface of uncoated nanoparticles is positive with a surface charge of +20 mV (Figure 2b). Adsorption of a polyanion results in changing the value of surface charge to a negative one. Surface charge alternation with sequential deposition of polycation and polyanion layers was observed for all used combinations except CMC/GelA where the ζ-potential of nanoparticles with a GelA outermost layer was slightly negative (Figure 2b). It confirms that the assembly takes place on the surface of the nanoparticles. At the same time, for weak polyelectrolyte or protein, surface charge values for the corresponding layer are only slightly positive or slightly negative despite their supposed high charge in solution at pH 6.0.[19,20] Aggregation of nanoparticles with a weak polyelectrolyte outermost layer increases the effective diameter and polydispersity (data not shown). Deposition of a strong polyelectrolyte as the next layer decreases aggregation of the particles (redisperse them).

As can be seen from the AFM and SEM images of coated nanoparticles (Figures 3c,e and b), the deposition of polyelectrolyte layers does not change significantly the nanoparticle's size or shape. Thickness of the four bilayer shell wall is estimated as 20 nm (based on QCM monitoring of PGA/PLL multilayer assembly on QCM electrode). The estimated mass of nanoparticles coated with $(PGA/PLL)_2$ or $(PGA/PLL)_4$ layers is almost the same as that of the initial nanoparticles. SEM confirms (Figure 5c) that the interior of gelatin nanoparticles with silica finished shell of $(DexS/PtS)_2/SiO_2$ composition remains gel-like and collapses after drying, leaving the upper layer of silica nanoparticles intact. The data from different methods ensure that adsorbed polyelectrolytes form a thin shell around nanoparticles with minimal penetration of the coating polyelectrolytes inside the nanoparticles.

In fact, about 0.13 g of PSS per 1 g of nanoparticles is necessary to saturate the first layer polyanion adsorption. This amount corresponds to about *ca.* 1 nm PSS layer thickness if a high effective surface area of gelatin nanoparticles and formation of a single polyanion layer are assumed. All of the above observations coincide with internal layering of LbL film with only

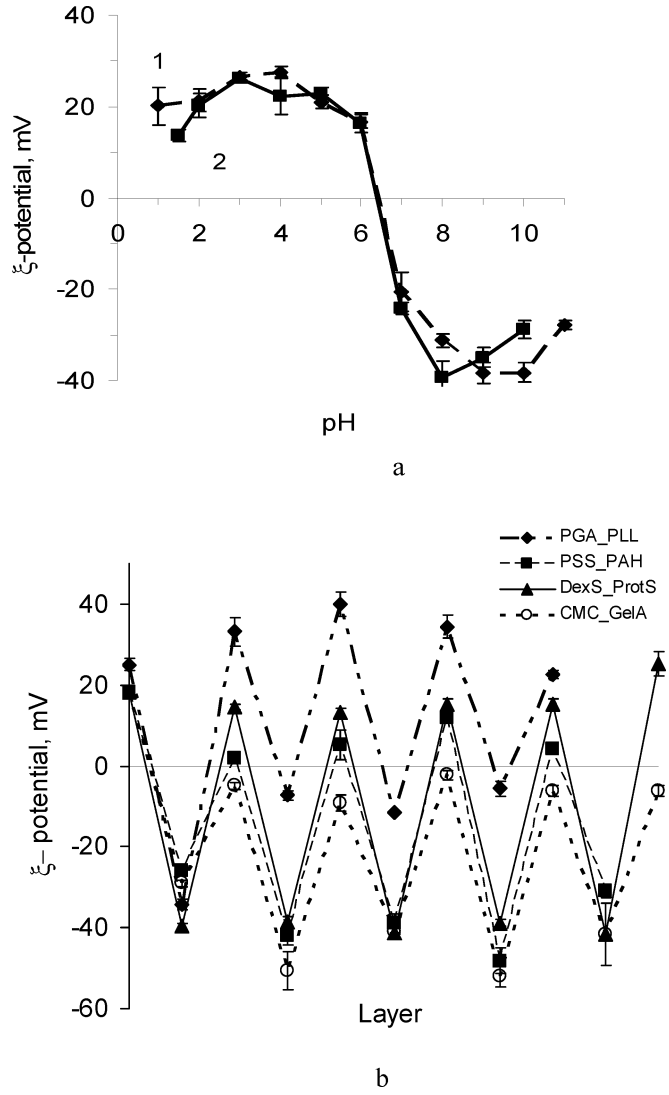

Figure 2. Surface charge of gelatin nanoparticles as functions of pH (a, 1- gelatin A, 2-gelatin B) and outermost polyelectrolyte layer (b, gelatin A, pH 6.0).

30−40% intermixing by height between adjacent layers as found by neutron reflectivity.[36,37]

Polyphenol Adsorption into Nanoparticles. Four different polyphenols (curcumin, EGCG, TA, and TF) were loaded by adsorption into the gelatin nanoparticles in order to evaluate nanoparticle loading efficiency (Figure 5). Adsorption of polyphenols with higher molecular weights and a larger number of phenolic −OH groups was found to be higher. The amount of theaflavin, the polyphenol with the highest molecular weight among those investigated, can reach 70% of the mass of nanoparticle solid material. Loading of tannic acid and EGCG is lower, while it is almost negligible for curcumin. The regularities of polyphenol adsorption correspond to general features of polyphenol−protein interaction and binding.[3,10−14,28−32] Most of the naturally occurring polyphenols, such as tannic acid, EGCG, gallic acid, cathechins *etc.* are well-known for their ability to precipitate salivary-rich proteins (albumin, gelatin, casein) from

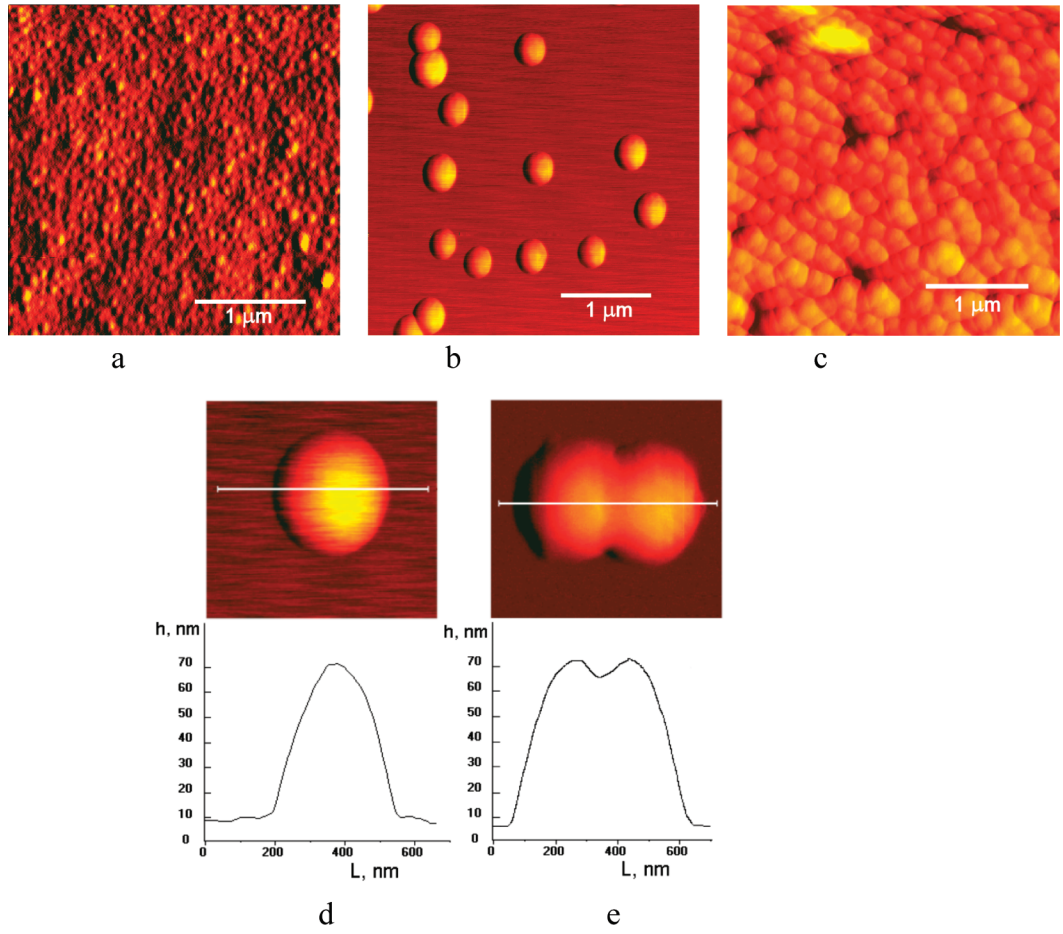

Figure 3. AFM images of 120 nm gelatin B (a, sample from 75% acetone) and 300 nm gelatin A (b−e, from water) uncoated (b,d) and coated with $(PGA/PLL)_2$ (c) and $(PGA/PLL)_4$ (e) shells. The corresponding profiles show sample elevation across the indicated lines.

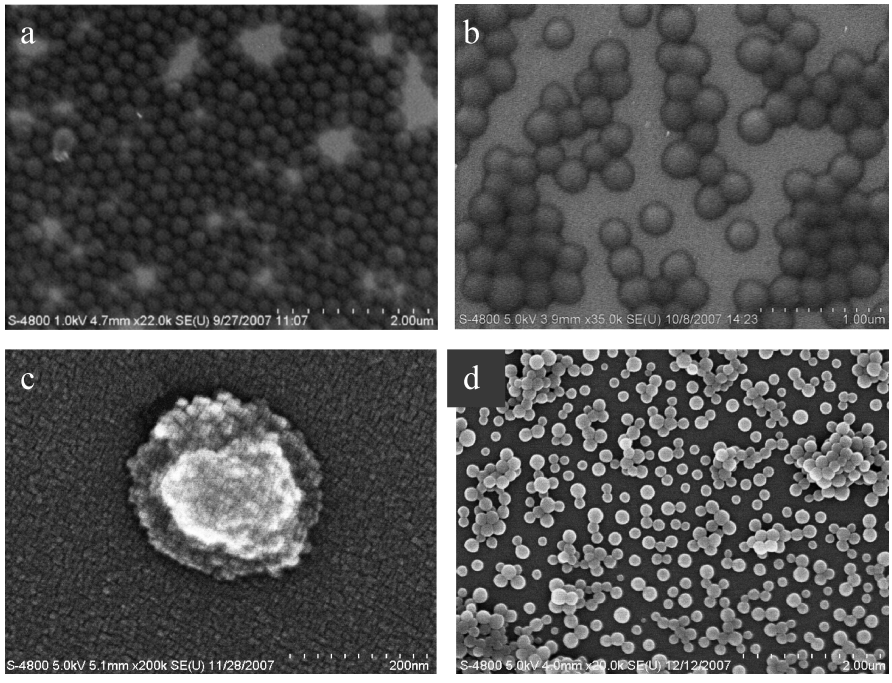

Figure 4. SEM images of 200 nm (a) and 300 nm (b−d) gelatin A nanoparticles: (a) uncoated, (b) coated with $(PGA/PLL)_2$ shells, (c) one nanoparticle coated with $(DexS/PtS)_2SiO_2$ shell, and (d) uncoated nanoparticles after loading EGCG.

aqueous solutions, although the binding strength highly varies and depends on protein/polyphenol pair. It is commonly accepted that the binding of gelatins by polyphenols is based mainly on hydrogen bonding between hydrophobic amino acid, mostly proline, residues and phenol rings of polyphenols. The presence of additional galloyl ester group(s) increases its binding.[3] However, interaction between polyphenols and proteins is a reversible and multistage process, which cannot be assigned to a single interaction reaction, as the complexes may redissolve while changing conditions (*e.g.*, pH).[30,31] We assume that, in the developed nanoparticles, the hydrophobic character of EGCG−gelatin interaction remains since glutaraldehyde cross-linking occurs *via* free amine groups of gelatin.

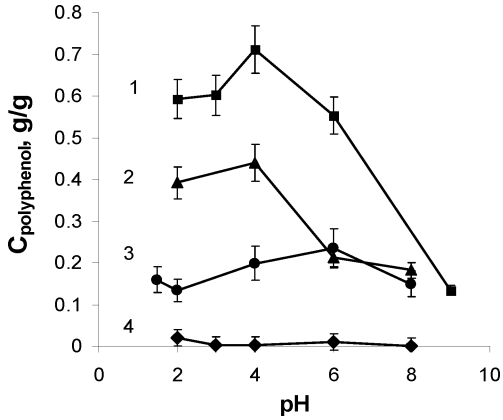

Figure 5. Total $C_{polyphenol}$ in suspension after loading theaflavins (1), tannic acid (2), EGCG (3), and curcumin (4) in 200 nm gelatin A (a) and 120 nm gelatin B (b) nanoparticles.

With increasing pH of loading, the amount of polyphenols adsorbed in nanoparticles decreases, probably due to the higher solubility of phenolate forms of the compounds[10−14,28−32] and changing the nanoparticle's interior charge. However, at pH higher than 8, all polyphenols became less stable and easily oxidized. This makes it difficult to test their adsorption at strongly basic conditions.

Loading of all polyphenols into gelatin A nanoparticles was higher than that for gelatin B nanoparticles. Different amino acid content of the gelatins can result in tailored hydrophobicity of the nanoparticles, affecting adsorption. Any influence of nanoparticle diameter on the value of EGCG loading in this set of experiments is unlikely because such influence is almost negligible for gelatin A nanoparticles of different diameters (Figure B, Supporting Information), which is within the range of experimental error. The diameter of EGCG-loaded nanoparticles is less than 200 nm (Figure 4d). This value is in agreement with their initial diameter estimated by SEM and ζ-potential measurements.

There is no evident influence of the polyelectrolyte layers on the EGCG concentration in the samples (Figure C, Supporting Information), and long 20−30 h adsorption gives similar loadings.

EGCG Release from Nanoparticles. Release of EGCG from uncoated gelatin A nanoparticles is very fast at all pH values and depends on conditions of loading and release. While the pH of EGCG loading is close to the pH value used for release experiments, a steady-state concentration of EGCG in solution is reached almost immediately, but only a part of EGCG appears to be in solution. When EGCG was adsorbed into nanoparticles at pH 4.0 and released at pH 7.5, the maximum concentration of EGCG was found 1 min after nanoparticle addition. The further decrease of EGCG concentration apparently indicates a slow system relaxation to a new equilibrium. It should be noted that the total EGCG concentration released after 3 h remains on the level of 90−95% of initial samples; the apparent loss is due to

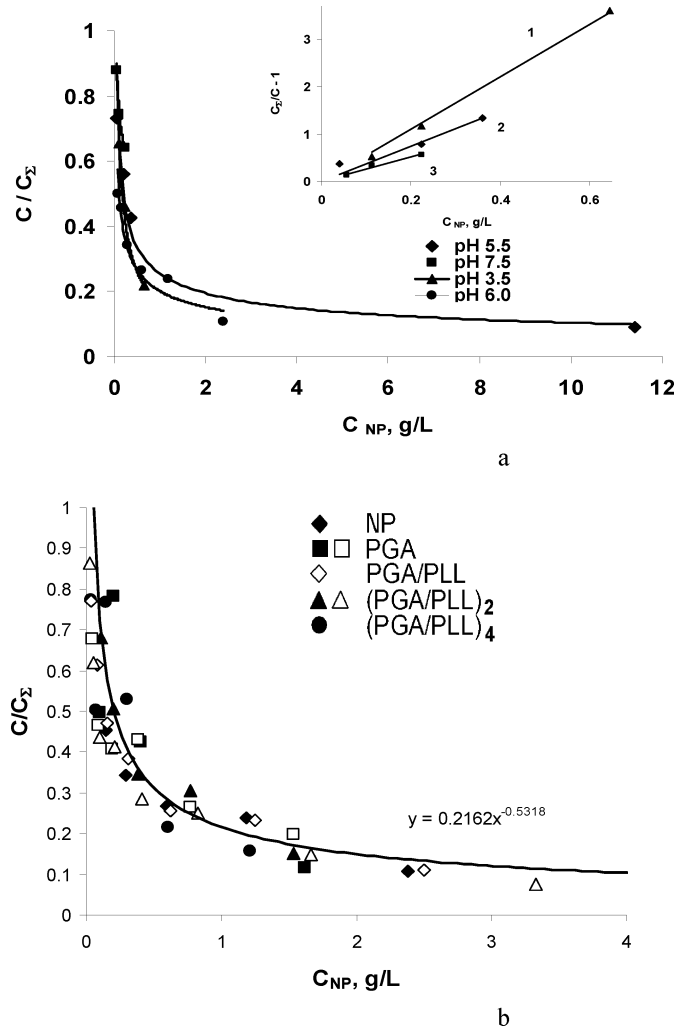

Figure 6. C/C_Σ as a function of nanoparticle concentration: (a) uncoated nanoparticles, (b) PGA/PLL-coated nanoparticles. The inset in (a) shows the curves in $C_\Sigma/C - 1$ *vs* C_{NP} coordinates.

the adsorption of the nanoparticles on the vial walls. It is worth mentioning that a similar release up to the level of 40−60% of encapsulated substance was previously observed for chitosan-tripolyphosphate nanoparticles containing tea extract and attributed to covalent binding of catechins to the matrix.[18]

In our case, if the nanoparticles are recollected and redispersed in water again, additional EGCG is released and new concentration equilibrium is reached (Figure D, Supporting Information). Almost 100% of EGCG was released after three such steps. It points toward a reversible type of EGCG−gelatin nanoparticle interaction and minimal covalent binding of EGCG with the gelatin matrix.

The ratio of EGCG concentration in supernatant (C) and its total concentration in the sample (C_Σ) does not linearly depend on the nanoparticle concentration (C_{NP}) (Figure 6). In a solution with high concentration of nanoparticles, EGCG is mostly in the nanoparticle's volume, while after addition of water, it immediately bursts out until new steady-state conditions are reached. At a

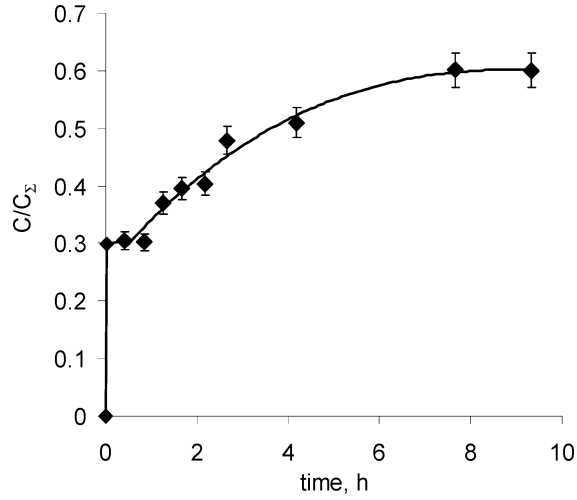

Figure 7. EGCG release from 275 nm gelatin A nanoparticles coated with PSS/PAH shells. C_{NP} = 0.22 g/L; pH of loading 6.8, pH of release 3.0. Time of loading = 48 h.

given pH, the data fit into a linear correlation $(C_\Sigma - C)/C = K_d \times C_{NP}$, where K_d is the distribution (partition) coefficient (Figure 7a, inset).

The calculated values of K_p are in range from 2.6 to 5.9 for different pH values used for loading and release (Table 1, Supporting Information). A higher K_d value corresponds to a higher amount of EGCG remaining in the nanoparticles. One can calculate that at pH 5.5 (K_d = 3.6) for uncoated gelatin nanoparticles with the total EGCG loading of 0.2 g per 1 g of nanoparticles in a suspension with C_{NP} = 2.5 g/L up to 90% of EGCG is adsorbed in nanoparticle volume, while the total volume of the nanoparticles in the solution is only around 1.5%.

Sustained Release of EGCG from LbL-Coated Nanoparticles. Gelatin nanoparticles with PSS/PAH bilayer loaded with 2.5 mg/mL EGCG demonstrate sustained release. This PSS/PAH shell consists only from one polyanion/polycation bilayer, and it cannot itself represent a dense diffusion barrier shell on the nanoparticle surface. Probably, the diffusion barrier structure involves deeper interaction of polyelectrolytes with gelatin core, similarly to the LbL protective barrier formation on soft PEG-assisted microcapsules for insulin delivery described earlier.[38] Nevertheless, we obtained slow release as compared with almost immediate 15 min EGCG release from uncoated gelatin nanoparticles. The maximum concentration of EGCG in solution was reached at 8 h (presented data are averaged over two different samples, Figure 7). The time interval is comparable to that observed for chitosan-tripolyphosphate nanoparticles.[18] Since the particles are stored in excess EGCG, we do see a baseline concentration at the first two points. Since the release volume contained nanoparticles, we observed that concentration equilibrium was reached. Using the biocompatible LbL shell of anionic dextran sulfate and cationic protamine sulfate was also possible but with less efficient release slowing.

Biological Activities of LbL-Coated Nanoparticles Containing EGCG. In order for EGCG nanoparticles to be a viable therapeutic option, it was necessary to ensure that EGCG nanoparticles function similar to free EGCG in a cell-culture model system. It has previously been shown that EGCG is capable of inhibiting numerous cell-signaling pathways, including the c-Met/HGF pathways. The secreted growth factor, HGF, activates the cell-membrane receptor, c-Met, leading to an increase in intracellular signaling and culminating in HGF-induced cell scattering, motility, and invasion. Invasion is one of the necessary steps leading to tumor metastasis, a lethal event in most cancer patients. We have demonstrated that free EGCG blocks HGF-induced scattering and activation of the c-Met receptor in a variety of tumor cell lines.[39] In order to determine if the biological activity of EGCG loaded into the nanoparticles was maintained after nanoparticle processing similar to free EGCG, the breast carcinoma cell line MDA-MB-231 was pretreated for varying times and concentrations with gelatin nanoparticles without EGCG, nanoparticles with EGCG, or free EGCG. HGF was added, and lysates were prepared 30 min later. Western blot analysis was performed using antibodies to detect phosphorylated c-Met and the downstream signaling molecules Akt and Erk, which are key molecules allowing signaling through the PI 3-kinase and Map Kinase pathways, respectively. Figure 8 illustrates that HGF induced a major increase in the phosphorylation of c-Met, Akt, and Erk. Free EGCG (5

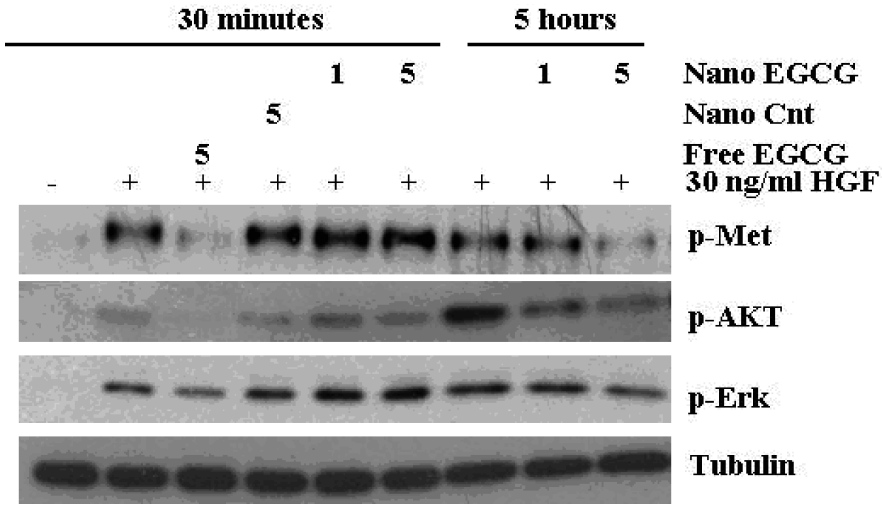

Figure 8. EGCG-containing nanoparticles inhibit HGF-induced c-Met signaling after prolonged preincubation. MDA-MB-231 cells were treated with either 5 μM free EGCG, 1 or 5 μM EGCG as coated nanoparticles, or the equivalent volume at 5 μM of control nanoparticles for 30 min or 5 h. The cells were pulsed with 30 ng/mL HGF for 30 min following the EGCG pretreatment time, and protein lysates were harvested. Western blot analysis was performed using the indicated antibodies to measure c-Met activation. Tubulin was used as a load control.

μM), at early time points, was able to inhibit HGF-induced c-Met, Akt, and Erk activation, as observed previously, while coated nanoparticles with and without EGCG were unable to inhibit HGF-induced signaling with short preincubation times. However, the EGCG-containing nanoparticles were capable of blocking HGF-induced signaling with longer preincubation times, thus demonstrating that the EGCG released from the nanoparticles maintains its biological activity, and that EGCG is being slowly released from the nanoparticles in concordance with the rate of EGCG release measured in Figure 7. Our long-range goal is to develop nanoparticles that will target tumor cells to release EGCG and other chemotherapeutic or targeted anticancer agents such as Erlotinib. As a first step, we have initiated animal studies to measure half-life of the nanoparticles and released EGCG. These pilot studies will lead to further studies that will address the potential therapeutic potential of slow release EGCG nanoparticles in an *in vivo* tumor mouse.

In conclusion, natural polyphenols with anticancer potential including EGCG, tannic acid, curcumin, and theaflavin were layer-by-layer encapsulated into gelatin-based 200 nm nanoparticles coated with organized 5−20 nm thick shells of polyelectrolytes (of different composition—from synthetic polyions to natural and biodegradable ones). The polyphenol loading was from 20 to 70 wt %. Factors affecting their release from the nanocapsules were investigated, and in the best case for EGCG, the release time reached 8 h (as compared with few minutes release for nonencapsulated nanoparticles). Nanoparticle-encapsulated EGCG retains its biological activity as both nanoparticles containing EGCG and free EGCG blocked HGF-induced intracellular signaling in the breast cancer cell line MBA-MD-231.

EXPERIMENTAL SECTION

Materials. Gelatin type A from porcine skin (GelA, Sigma G1890, 300 Bloom) or gelatin type B from bovine skin (GelB, Sigma G9391, 225 Bloom), glutaraldehyde (25% solution, Grad II, Sigma), acetone (Richard-Allan, scientific grade ACS), 2,2′-azinobis(3-ethylbenzothiazoline-6-sulfonic acid)diammonium salt (ABTS), and potassium persulfate ($K_2S_2O_8$) were used without additional purification.

Polyelectrolytes, polystyrene sulfonate (PSS), polyallylamine hydrochloride (PAH), poly-L-glutamic acid (PGA) and poly-L-lysine (PLL), dextran sulfate (DexS), protein protamine sulfate (ProtS), and polyphenols, curcumin, epigallocatechin gallate (EGCG), tannic acid (TA), and mixture of theaflavin and theaflavin gallate (TF) were bought from Sigma-Aldrich and used as received.

Nanoparticle Preparation. Gelatin nanoparticles were prepared using a modified two-step desolvation method.[33−35] In a typical experiment, 1.25 g of gelatin was dissolved in 25 mL of DI water by gentle heating to 50 °C, then 25 mL of acetone was rapidly added to the solution and slightly shaken. After exactly 2 min, a white colored supernatant was discharged. The gel-like precipitate was redissolved in 25 mL of water at light heating to 50 °C, and pH was adjusted with HCl. The range of pH tested was between 1.5 and 5. Then under constant stirring at 40 °C, 75 mL of acetone was slowly added during 15 min (less than 3 mL/min). The white milk-like solution started to form when 55−60 mL of acetone was introduced into the mixture (pH 3.0). Immediately after addition of acetone, 0.2 mL of 25% glutaraldehyde was admixed to the stirring mixture. Stirring continued for 1 h, followed by overnight incubation at room temperature, after which it was placed into plastic tubes and kept at +2 °C until further study. Since the amount of glutaraldehyde used to cross-link the nanoparticles is very small, we assume that it completely reacts with nanoparticles and there is no free glutaraldehyde in the mixture; no additional steps were done to quench it.

The prepared suspension was divided into 2 mL aliquots, and gelatin nanoparticles were separated from the supernatant by centrifugation at 6000−7000 rpm for 20 min and washed with 75% aqueous acetone three times. Finally, to concentrate the sample, the content of each tube was resuspended in 0.5 mL of 75% acetone and combined. The concentration of solid material in the suspension was usually as high as 30−40 mg/mL and was estimated for each batch separately, if needed. The nanoparticles as a stable suspension of white or yellowish white color were kept at +2 °C until used. Nanoparticles prepared at pH 2.5−3.0 on the second desolvation stage were used for all further studies.

LbL Shell Assembly on Gelatin Nanoparticles. For polyelectrolyte encapsulation of gelatin nanoparticles, 0.4 mL of a 3 mg/mL solution of polyanion (PSS, PGA, DexS), polycation (PAH, PLL), or protamine sulfate (PtS) at pH 6.0 was added sequentially to 1.5 mL of an aqueous suspension containing 15−20 mg/mL gelatin A nanoparticles. After 30 min adsorption of each layer, the nanoparticles were washed with DI water three times. The corresponding polyanion was always deposited as the first layer on positive gelatin nanocores. Deposition of each layer was monitored with ζ-potential measurements. For SEM imaging, one layer of SiO_2 nanoparticles (7 nm) was deposited on the top of gelatin particles coated with a $(DexS/PtS)_2$ shell. The detailed procedure for formation of LbL shells on microcores can be found elsewhere.[17,18,20]

To estimate the amount of polyanion that can be adsorbed by the nanoparticles, in one of the experiments, adsorption of PSS was carried out on 10 mg/mL gelatin A nanoparticles from a 0.2 mg/mL PSS supernatant in a stepwise manner, and the amount of PSS remaining in solution was estimated using UV−visible spectroscopy.

Discoloration of $ABTS^{+\bullet}$ by Polyphenols in Solution. A stock solution of cation radical ABTS ($ABTS^{+\bullet}$) was prepared as described.[40] Eighty-eight microliters of 0.14 M $K_2S_2O_8$ was added to 5 mL of 7×10^{-3} M ABTS aqueous solution and left overnight at room temperature. The obtained stock solution of intensive blue-green color was kept protected from light at +2 °C. The stock solution was diluted with DI water (pH 6.5) immediately before use in such a way that the absorbance at 734 nm (A_0) was equal to 1.40 ± 0.05 (l = 1.0 cM, $\varepsilon = 1.4 \times 10^4$ M^{-1} cM^{-1}.[35] The difference of A_0 in separate series was not higher than ±0.05.

To calibrate the $ABTS^{+\bullet}$ assay, initially designed to evaluate antioxidant properties of phenolic substances,[40−44] 10−250 μL of 0.1−3.0 mg/mL solution of different polyphenols (curcumin, EGCG, TA, TF) or gelatin was added to 2.0 or 3.0 mL of an aqueous $ABTS^{+\bullet}$ solution (pH 6.5) as above and thoroughly mixed. Absorbance of the mixture at 734 nm (A_t) was read spectrophotometrically (an Agilent 8453 spectrometer). To evaluate the effect of sample dilution on A_t, a series of blank experiments, where pure DI water was added in the place of a polyphenol containing sample, was carried out, and the results were used to estimate A_t changes. In a separate series of experiments to determine the time interval necessary to complete the polyphenol reaction with $ABTS^{+\bullet}$, absorbance of the mixture at 734 nm was followed in time for 120 min with reading intervals 10 s under constant stirring of the sample. The concentration of each polyphenol was evaluated from the absorbance change after 90 min using experimentally obtained calibration coefficient.

Discoloration of $ABTS^{+\bullet}$ by Gelatin Nanoparticles Containing Polyphenols. To determine the amount of polyphenols loaded in gelatin nanoparticles, 5−20 μL of EGCG-containing sample was added to 2.0−3.0 mL of the aqueous $ABTS^{+\bullet}$ solution (pH 6.5) as

above and thoroughly mixed. The decrease of absorbance at 734 nm (A_t) after 90 min was converted into polyphenol concentration.

The effect of nanoparticles on the results of EGCG determination with the $ABTS^{+\bullet}$ method was evaluated in an additional series of experiments. Solutions containing 0.5 mg/mL of EGCG and nanoparticles in the range of 0−0.75 mg/mL were prepared and tested. Nanoparticles were separated from the reaction volume before the addition of the ABTS reagent due to spectral confounding.

Loading of EGCG and Other Polyphenols into Gelatin Nanoparticles. Loading of EGCG into uncoated nanoparticles by adsorption of the polyphenol from its concentrated aqueous solution was compared at different pH values. Typically, 0.4 mL of 10.0 mg/mL EGCG was mixed with 0.4 mL water, and the pH was adjusted to the value under investigation with HCl or NaOH. Then 0.2 mL of nanoparticle suspension was added at room temperature and mixed. After 60 min, EGCG-loaded nanoparticles were separated from supernatant by centrifugation at 6000−7000 rpm for 20 min; the supernatant was replaced with 2.0 mL of DI water (pH 6.5), and the nanoparticles were resuspended; the washing procedure was repeated, and then the loaded nanoparticles were diluted in 0.25 mL of DI water. The concentration of EGCG in the sample was determined using the $ABTS^{+\bullet}$ assay; the concentration of solid residue using QCM. EGCG was loaded into nanoparticles modified with different polyelectrolyte layers using the same procedure as above except that the nanoparticles were initially suspended in DI water. A blank sample with uncoated nanoparticles from the same original sample was used as a control in each experimental series. For extended release studies, the nanoparticles were encapsulated with a 3 mg/mL PAH and PSS. Two layers were adsorbed onto the nanoparticles. Three hundred microliters of 5 mg/mL EGCG was adsorbed onto 300 μL of the coated nanoparticles for 48 h at pH 6.8. Release studies were performed at pH 3 using the adsorbed sample by adding 100 μL of the loaded sample to 5 mL of DI under constant stirring action (~200 rpm). Aliquots were taken with respect to time for 10 h.

Tannic acid adsorption into gelatin nanoparticles followed the exact procedure for EGCG. Taking into account solubility of other polyphenols, we modified the procedure as follows. Theaflavin was loaded from a 1.6 mg/mL supernatant containing 25% of acetone. Curcumin was adsorbed from a 0.08 mg/mL supernatant containing 25% ethanol and 12.5% acetone. In all cases, the polyphenols were in excess.

EGCG Release from Gelatin Nanoparticles. In a typical release experiment, 0.1−0.2 mL of EGCG-loaded sample with known initial concentrations of EGCG and nanoparticles was added to 5−10 mL of DI water with given pH and mixed. Immediately after mixing, with 10−60 min intervals, 0.2 mL aliquots were taken with a syringe and the solution was passed through a Anotop or Pall syringe filter with 0.2 μm cutoff. The filtrate was collected and tested for EGCG concentration. In each experiment, the total concentration of EGCG in the reaction mixture, after the release experiment was complete, was determined.

To evaluate the percentage of EGCG released as a function of nanoparticles concentration, a suspension of EGCG-loaded nanoparticles was added to different volumes of DI water and, after 20 min, the supernatant was separated by passing the sample through the 0.2 μm filter and the concentration of EGCG in it was determined using the $ABTS^{+\bullet}$ assay.

Western Blotting. MDA-MB-231 cells were obtained from ATCC and grown in DMEM (Cellgro; Herndon, VA) and supplemented with 10% FBS (Gemini Bio-Products; West Sacramento, CA) and 1% penicillin/streptomycin (Cellgro). MDA-MB-231 cells were plated at 90% confluence in a 24 well plate. The following day, MDA-MB-231 cells were treated with either 5 μM free EGCG, 1 or 5 μM EGCG as coated nanoparticles, or the equivalent volume at 5 μM of control nanoparticles for 30 min or 5 h. The cells were pulsed with 30 ng/mL HGF (hepatocyte growth factor, Calbiochem; 30 ng/mL) for 30 min immediately upon EGCG treatment or 30 min prior to the 5 h time point. Protein lysates were harvested in 125 μL boiling Laemmli sample buffer (125 mM Tris; 4% SDS; 0.01% bromophenol blue; 30% sucrose; 5% β-mercaptoethanol). Ten microliters of the lysates was run on a 10% SDS-PAGE gel, transferred to PVDF membrane (Pall Corporation; Pensacola, FL), blocked with 5% milk in TBS-T (50 mM Tris-HCl, pH 7.5 150 mM NaCl, 0.1% Tween-20) for 1 h, and probed with antibodies to the proteins listed below overnight at 4 °C. The following day, the membranes were washed with TBS-T and probed with horseradish peroxidase conjugated secondary antibodies (GE Healthcare; Buckinghamshire, UK). The membranes were washed with TBS-T, and the signal was detected with ECL Plus (GE Healthcare). Antibodies used included phospho-Erk, phospho-Akt, phospho-c-Met (Cell Signaling Technology; Beverly, MA), and tubulin (Neomarkers; Freemont, CA).

Characterization of Nanoparticles. The measurements of nanoparticle hydrodynamic diameter and ζ-potential were carried out on a ZetaPlus Brookheaven microelectrophoretic instrument in water. For the measurements, 0.1 mL of nanoparticle suspension was redispersed in 2 mL of water. To determine the isoelectric point of gelatin nanoparticle, the diluted solutions were kept 24 h before the measurements.

SEM images were taken on a Hitachi S-4800 scanning electron microscope. The samples for SEM imaging were typically prepared by applying 2−5 μL of diluted nanoparticle suspension in water (gelatin A) or ethanol (gelatin B) on the surface of Si template followed by overnight drying. To enhance image quality, sample surface was spattered with 2 nm layer of iridium.

AFM images were obtained using a Q-Scope 250 Quesant instrument in intermittent-contact mode. Samples were prepared as above on freshly cleaved mica.

The concentration of solid residue in a gelatin nanoparticle sample was estimated using quartz crystal microbalance (QCM) technique. Typically, 2−5 μL of each sample was placed on one side of a precleaned horizontally maintained quartz resonator; the drop was dried at room temperature in air to a steady weight (~30 min), and the frequency changes of the resonator were monitored using a USI-System, Japan, 9 MHz QCM instrument with the accuracy of ±1 Hz. The mass of deposited material was recalculated from the frequency shift according to the Sauerbrey equation: Δm (ng) $= -0.84\Delta F$ (Hz). Then the resonator was replaced, and the procedure was repeated. For each sample, two or four independent runs were done with different resonators, and the results were averaged. Typical experimental deviation between different runs was less than 15%. Dry gelatin nanoparticles containing EGCG were obtained using a Modulyo freeze drier. The samples were frozen in liquid nitrogen.

Acknowledgment. This work is supported by Louisiana NSF-EPSCoR #34768 and NSF #0508560 grants to Y.L., and an NIH grant, R01-CA104242, to J.C. Any opinions, findings, and conclusions or recommendations expressed in this material are those of the authors and do not necessarily reflect the view of the National Science Foundation or National Institutes of Health.

Supporting Information Available: Gelatin A nanoparticle diameter and polydispersity as a function of pH on the second desolvation stage. C_{EGCG} in uncoated gelatin A nanoparticles of different diameters. Concentration of EGCG in nanoparticles coated with different number of PGA/PLL bilayers. Three-stage release of EGCG from gelatin nanoparticles. K_d as a function of pH and nanoparticles coating. This material is available free of charge *via* the Internet at http://pubs.acs.org.

REFERENCES AND NOTES

1. Haslam, E. Natural Polyphenols (Vegetable Tannins) as Drugs: Possible Modes of Action. *J. Nat. Prod.* **1996**, *59*, 205–215.
2. Quideau, S.; Feldman, K. S. Ellagitannin Chemistry. *Chem. Rev.* **1996**, *96*, 475–503.
3. Bennick, A. Interaction of Plant Polyphenols with Salivary Proteins. *Crit. Rev. Oral Biol. Med.* **2002**, *13*, 184–196.
4. Adhami, V. M.; Mukhtar, H. Anti-oxidants from Green Tea and Pomegranate for Chemoprevention of Prostate Cancer. *Mol. Biotechnol.* **2007**, *37*, 52–57.
5. Bettuzzi, S.; Brausi, M.; Rizzi, F.; Castagnetti, G.; Peracchia, G.; Corti, A. Chemoprevention of Human Prostate Cancer by Oral Administration of Green Tea Catechins in Volunteers with High-Grade Prostate Intraepithelial Neoplasia: A Preliminary Report from a One Year Proof of Principle Study. *Cancer Res.* **2006**, *66*, 1234–1240.

6. Surh, Y. J. Cancer Chemoprevention with Dietary Phytochemicals. *Nat. Rev. Cancer* **2003**, *3*, 768–780.
7. Ravi Kumar, M. N. V.; Muzzarelli, R. A. A.; Muzzarelli, C.; Sashiwa, H.; Domb, A. J. Chitosan Chemistry and Pharmaceutical Perspectives. *Chem. Rev.* **2004**, *104*, 6017–6084.
8. Vinogradov, S. V. Colloidal Microgels in Drug Delivery Applications. *Curr. Pharm. Des.* **2006**, *12*, 4703–4712.
9. Al-Tahami, K.; Smart, S. J. Polymer Based Delivery Systems for Peptides and Proteins. *Recent Pat. Drug Delivery Formulation* **2007**, *1*, 65–71.
10. Calderon, P.; Van Buren, J.; Robinson, W. B. Factors Influencing the Formation of Precipitates and Hazes by Gelatin and Condensed and Hydrolyzable Tannins. *J. Agric. Food Chem.* **1968**, *16*, 479–482.
11. Gámiz-Gracia, L.; Luque de Castro, M. D. Development and Validation of a Flow-Injection Method for the Determination of Albumin Tannate, the Active Component of a Pharmaceutical Preparation. *J. Pharm. Biomed. Anal.* **1997**, *15*, 447–452.
12. Osawa, R. S. J.; Walsho, T. P. Effects of Acidic and Alkaline Treatments on Tannic Acid and Its Binding Property to Protein. *J. Agric. Food Chem.* **1999**, *41*, 704–707.
13. Barik, A.; Priyadarsini, K. I.; Mohan, H. Photophysical Studies on Binding of Curcumin to Bovine Serum Albumin. *Photochem. Photobiol.* **2003**, *77*, 597–603.
14. Yi, K.; Cheng, G.; Xing, F. Gelatin/Tannin Complex Nanospheres via Molecular Assembly. *J. Appl. Polym. Sci.* **2006**, *101*, 3125.
15. Shutava, T.; Prouty, M.; Kommirredy, D.; Lvov, Y. pH-Responsive Decomposable Layer-by-Layer Nanofilms and Capsules on the Basis of Tannic Acid. *Macromolecules* **2005**, *38*, 2850–2858.
16. Shutava, T. G.; Lvov, Y. M. Nanoengineered Microcapsules of Tannic Acid and Chitosan for Protein Encapsulation. *J. Nanosci. Nanotechnol.* **2006**, *6*, 1655–1661.
17. Italia, J. L.; Datta, P.; Ankola, D. D.; Kumar, M. N. V. Ravi Nanoparticles Enhance Per Oral Bioavailability of Poorly Available Molecules: Epigallocatechin Gallate Nanoparticles Ameliorates Cyclosporine Induced Nephrotoxicity in Rats at Three Times Lower Dose Than Oral Solution. *J. Biomed. Nanotechnol.* **2008**, *4*, 304–312.
18. Hu, B.; Pan, C.; Sun, Y.; Hou, Z.; Ye, Y.; Hu, B.; Zeng, X. Optimization of Fabrication Parameters To Produce Chitosan-Tripolyphosphate Nanoparticles for Delivery of Tea Catechins. *J. Agric. Food Chem.* **2008**, *56*, 7451–7458.
19. McShane, M.; Lvov, Y. Layer-by-Layer Electrostatic Self-Assembly In *Dekker Encyclopedia of Nanoscience & Nanotechnology*; Schwartz, J., Contescu, C., Eds.; Marcel Dekker: New York, 2004; pp 1−21.
20. Ai, H.; Jones, S. A.; Lvov, Y. M. Biomedical Application of Electrostatic Layer-by-Layer Nano-assembly of Polymers, Enzymes, and Nanoparticles. *Cell Biochem. Biophys.* **2003**, *39*, 23–43.
21. Zahr, A. S. Pishko MV Encapsulation of Paclitaxel in Macromolecular Nanoshells. *Biomacromolecules* **2007**, *8*, 2004–2010.
22. Zhou, J.; Moya, S.; Ma, L.; Gao, C.; Shen, J. Polyelectrolyte Coated PLGA Nanoparticles: Templation and Release Behavior. *Macromol. Biosci.* **2009**, *4*, 326–335.
23. Ai, H.; Pink, J. J.; Shuai, X.; Boothman, D. A.; Gao, J. Interactions between Self-Assembled Polyelectrolyte Shells and Tumor Cells. *J. Biomed. Mater. Res.* **2005**, *73A*, 303–312.
24. Qiu, X.; Leporatti, S.; Donath, E.; Möhwald, H. Studies on the Drug Release Properties of Polysaccharide Multilayers Encapsulated Ibuprofen Microparticles. *Langmuir* **2001**, *17*, 5375–5380.
25. Kommareddy, S.; Amiji, M. Antiangiogenic Gene Therapy with Systemically Administered sFlt-1 Plasmid DNA in Engineered Gelatin-Based Nanovectors. *Cancer Gene Ther.* **2007**, *14*, 488–498.
26. Kaul, G; Amiji, M. Tumor-Targeted Gene Delivery Using Poly(ethylene glycol)-Modified Gelatin Nanoparticles: *In Vitro* and *In Vivo* Studies. *Pharm. Res.* **2005**, *22*, 951–961.
27. Kommareddy, S; Amiji, M. Biodistribution and Pharmacokinetic Analysis of Long-Circulating Thiolated Gelatin Nanoparticles Following Systemic Administration in Breast Cancer-Bearing Mice. *J. Pharm. Sci.* **2007**, *96*, 397–407.
28. Jöbstl, E.; Howse, J. R.; Fairclough, J. P. A.; Williamson, M. P. Noncovalent Cross-Linking of Casein by Epigallocatechin Gallate Characterized by Single Molecule Force Microscopy. *J. Agric. Food Chem.* **2006**, *54*, 4077–4081.
29. Charlton, A. J.; Baxter, N. J.; Khan, M. L.; Moir, A. J. G.; Haslam, E.; Davies, A. P.; Williamson, M. P. Polyphenol/Peptide Binding and Precipitation. *J. Agric. Food Chem.* **2002**, *50*, 1593–1601.
30. Baxter, N. J.; Lilley, T. H.; Haslam, E.; Williamson, M. P. Multiple Interactions between Polyphenols and a Salivary Proline-Rich Protein Repeat Result in Complexation and Precipitation. *Biochemistry* **1997**, *36*, 5566–5577.
31. Pascal, C.; Poncet-Legrand, C. L.; Imberty, A.; Gautier, C.; Sarni-Manchado, P.; Chenynier, V. R.; Vernhet, A. Interactions Between a Non Glycosylated Human Proline-Rich Protein and Flavan-3-ols are Affected by Protein Concentration and Polyphenol/Protein Ratio. *J. Agric. Food Chem.* **2007**, *55*, 4895–4901.
32. Naurato, N.; Wong, P.; Lu, Y.; Wroblewski, K.; Bennick, A. Interaction of Tannin with Human Salivary Histatins. *J. Agric. Food Chem.* **1999**, *47*, 2229.
33. Zwiorek, K.; Klöckner, J.; Wanger, E.; Coester, C. Gelatin Nanoparticles as a New and Simple Gene Delivery System. *J. Pharm. Pharm. Sci.* **2004**, *7*, 22–28.
34. Zillies, J. C.; Zwiorek, K.; Winter, G.; Coester, C. Method for Guantifying the PEGylation of Gelatin Nanoparticle Drug Carrier Systems Using Asymmetrical Flow Field-Flow Fractionation and Refractive Index Detection. *Anal. Chem.* **2007**, *79*, 4574–4580.
35. Cumper, C. W. N.; Alexander, A. E. the Viscosity and Rigidity of Gelatin in Concentrated Aqueous Systems. I. Viscosity. *Aus. J. Sci. Res., Ser. A: Phys. Sci.* **1952**, *5*, 146–152.
36. Jomaa, H. W.; Schlenoff, J. B. Salt-Induced Polyelectrolyte Interdiffusion in Multilayered Films: A Neutron Reflectivity Study. *Macromolecules* **2005**, *38*, 8473–8480.
37. Kharlampieva, E.; Kozlovskaya, V.; Ankner, J. F.; Sukhishvili, S. A. Hydrogen-Bonded Polymer Multilayers Probed by Neutron Reflectivity. *Langmuir* **2008**, *24*, 11346–11349.
38. Rashba-Step, J.; Darvari, R.; Kelly, J.; Shutava, T.; Lvov, Y.; Scott, T. Surface Modification of PROMAXX Microparticles. In Proceedings of 33rd Annual Controlled Release Society Meeting, Vienna, Austria 2006; pp 78−80.
39. Bigelow, R. L. H.; Cardelli, J. A. The Green Tea Catechins, (−)-Epigallocatechin-3-gallate (EGCG) and (−)-Epicatechin-3-gallate (ECG), Inhibit HGF/Met Signaling in Immortalized and Tumorigenic Breast Epithelial Cells. *Oncogene* **2006**, *25*, 1922–1930.
40. Re, R.; Pellegrini, A.; Proteggente, A.; Pannala, A.; Yang, M.; Rice-Evans, C. Antioxidant Activity Applying an Improved ABTS Radical Cation Decolorization Assay. *Free Radical Biol. Med.* **1999**, *26*, 1231–1237.
41. Riedl, K. M.; Hagerman, A. E. Tannin−Protein Complexes as Radical Scavengers and Radical Sinks. *J. Agric. Food Chem.* **2001**, *49*, 4917–4923.
42. Campos, A. M.; Sotomayor, C. P.; Pino, E.; Lissi, E. A. A Pyranine Based Procedure for Evaluation of the Total Antioxidant Potential (TRAP) of Polyphenols. A Comparison with Closely Related Methodologies. *Biol. Res.* **2004**, *37*, 287–292.
43. Takebayashi, J.; Tai, A.; Yamamoto, I. pH-Dependent Long-Term Radical Scavenging Activity of AA-2G and 6-Octa-AA-2G against 2,2′-Azinobis(3-ethylbenzothiazoline-6-sulfonic acid) Radical Cation. *Biol. Pharm. Bull.* **2003**, *26*, 1368–1370.
44. Jonson, K. S. Plant Phenolics Behave as Radical Scavengers in the Context of Insect (*Manduca sexta*) Hemolymph and Midgut Fluid. *J. Agric. Food Chem.* **2005**, *53*, 10120–10160.